

Signatures of minor mergers in Milky Way-like disc kinematics: Ringing revisited

Facundo A. Gómez^{1,2*}, Ivan Minchev³, Álvaro Villalobos⁴,
Brian W. O’Shea^{1,2,5} & Mary E. K. Williams³

¹ *Department of Physics and Astronomy, Michigan State University, East Lansing, MI 48824, USA*

² *Institute for Cyber-Enabled Research, Michigan State University, East Lansing, MI 48824, USA*

³ *AIP, An der Sternwarte 16, 14482 Potsdam, Germany*

⁴ *INAF-Osservatorio Astronomico di Trieste, Via Tiepolo 11, I-34143 Trieste, Italy*

⁵ *Lyman Briggs College, Michigan State University, East Lansing, MI 48825, USA*

ABSTRACT

By means of N -body simulations we study the response of a galactic disc to a minor merger event. We find that non-self-gravitating, spiral-like features are induced in the thick disc. As we have shown in a previous work, this “ringing” also leaves an imprint in velocity space (the u - v plane) in small spatial regions, such as the solar neighbourhood. As the disc relaxes after the event, clumps in the u - v plane get closer with time, allowing us to estimate the time of impact. In addition to confirming the possibility of this diagnostic, here we show that in a more realistic scenario, the in-fall trajectory of the perturber gives rise to an azimuthal dependence of the structure in phase-space. We also find that the space defined by the energy and angular momentum of stars is a better choice than velocity space, as clumps remain visible even in large local volumes. This makes their observational detection much easier since one need not be restricted to a small spatial volume. We show that information about the time of impact, the mass of the perturber, and its trajectory is stored in the kinematics of disc stars.

Key words: galaxies: formation – galaxies: kinematics and dynamics – methods: analytical – methods: N -body simulations

1 INTRODUCTION

The present day spatial distribution, motion, ages and chemical abundances of stars contain important information about how galaxies form and evolve (Freeman & Bland-Hawthorn 2002). Substructure in these distributions has been observed, especially in the Milky Way (e.g. Ibata, Gilmore & Irwin 1994; Helmi et al. 1999; Newberg et al. 2002; Ibata et al. 2003; Yanny et al. 2003; Navarro, Helmi & Freeman 2004; Belokurov et al. 2006; Helmi et al. 2006; Starkenburg et al. 2009; Klement et al. 2009; Williams et al. 2009, 2011), but also in other galaxies (e.g. Ibata et al. 2001; Chapman et al. 2008; Martínez-Delgado et al. 2008, 2009; McConnachie et al. 2009). This substructure can arise from a variety of different physical mechanisms. Examples are the disruption of open clusters (Eggen 1996), the dynamical effects induced by non-axymmetric components of a galaxy, such as a bar

or self-gravitating spiral arms (see e.g. Dehnen 2000; Fux 2001; Minchev & Quillen 2008; Antoja et al. 2009; Minchev et al. 2010; Quillen et al. 2011), or debris from satellite galaxies that were accreted by their more massive host (e.g. Helmi & White 1999; Helmi & de Zeeuw 2000; Bullock & Johnston 2005; Font et al. 2006; Sales et al. 2008; Michel-Dansac et al. 2011). Another possible mechanism, introduced by Minchev et al. (2009, hereafter M09), is related to the response of a galactic disc to the tidal interaction with a satellite galaxy as it merges. Thanks to dynamical friction, relatively massive satellites can reach the centre of the disc before being completely disrupted by the tidal field (Binney & Tremaine 2008). M09 showed that the sudden energy kick imparted by the gravitational potential of the satellite, as it crosses the plane of the disc, can strongly perturb the velocity field of disc stars located in local volumes such as the Solar Neighbourhood. These perturbations can be observed in the u - v plane as arc-like features travelling in the direction of positive v , where u and v are the radial and tangential velocity components. This

* Email: fgomez@pa.msu.edu

mechanism, known as “ringing”, could explain the presence of high velocity streams observed in the Solar Neighbourhood, such as the Arcturus stream (Williams et al. 2009). Furthermore, as shown by Quillen et al. (2009), minor mergers can also induce radial mixing in the outer disc, thus partially explaining the lack of correlation between age and metallicity observed in the Milky Way’s thick disc (see Villalobos 2009, and references therein).

An important limitation in the M09 analysis is the extent of the local volume that can be explored to search for signatures of ringing in the u - v plane. As the depth of the volume is increased, a progressively larger number of density waves is included. This causes the waves to interfere, wiping out the substructure previously observed in this projection of phase-space. This not only places constraints on the size of stellar samples that can be explored to search for signatures of ringing in the Solar Neighbourhood, but also makes studying this mechanism in fully self-consistent N -body simulations unfeasible. Note that to resolve local volumes as small as, e.g., 100 pc, an extremely large particle resolution is required. Thus, in M09 only relatively simple high-resolution 2D simulations of massless test-particles were performed to explore this problem.

In this paper we show that the space of energy and angular momentum is much more suitable for identifying the signatures of ringing in a galactic disc. In this projection of phase-space much larger local volumes can be explored without erasing the substructure associated with ringing (Section 3). This allows us to analyse a set of fully self-consistent N -body simulations of a merger between a relatively massive satellite galaxy and a pre-existing thin disc (Section 4). We briefly describe our simulations in Section 2. In Section 5 we summarise our results and discuss its application to currently available as well as forthcoming full 6D phase-space samples of thick disc stars in the Solar vicinity.

2 SIMULATIONS

Two types of numerical simulations are studied in this work. First, we analyse a two dimensional massless test-particle simulation of an unrelaxed stellar galactic disc, as described by M09. In this model, a flat rotational velocity profile is considered, with a value of 220 km s^{-1} at 7.8 kpc from the galactic centre. The disc follows an exponential density profile with a scale-length of 3 kpc. Initial velocities for the particles are drawn from Gaussian distributions in the u and v directions. In particular, the standard deviation in the radial direction is set at $\sigma_u = 50 \text{ km s}^{-1}$. To emulate a population that is unrelaxed, velocities are purposely chosen so that particles are unevenly distributed in their radial oscillation. A total of 7×10^6 test-particles were used to represent the disc. For more details, we refer the reader to M09.

Second, we analyse a set of fully self-consistent N -body simulations of the merger between a satellite galaxy and a pre-existing galactic thin disc. Most of these simulations were first presented by Villalobos & Helmi (2008, hereafter, VH08) to study the formation of a galactic thick disc due to the heating induced by the merger event. In particular, the simulations considered in this work are those referred as “ $z = 1$ ” in VH08, which were set up to emulate a merger event that could have given rise to

Table 1. Initial properties of the three N -body simulations analysed in this work.

Host’s DM halo				
Virial mass, $M_{\text{host}}^{\text{DM}}$	5.07×10^{11}			$[M_{\odot}]$
Virial radius	122.22			[kpc]
Concentration	6.56			
Host’s stellar disc				
Mass, $M_{\text{host}}^{\text{stellar}}$	1.2×10^{10}			$[M_{\odot}]$
Scale length, R_d	1.65			[kpc]
Scale height, z_0	0.165			[kpc]
Satellite’s DM halo	$f = 20\%$	15%	10%	
Virial mass, $M_{\text{sat}}^{\text{DM}}$	1.01	0.75	0.5	$10^{11} [M_{\odot}]$
Virial radius	71.35	64.65	56.63	[kpc]
Concentration	8.09	8.41	8.86	
Satellite’s stellar bulge				
Mass, $M_{\text{sat}}^{\text{stellar}}$	2.4	1.8	1.2	$10^9 [M_{\odot}]$
Scale radius, r_b	0.709	0.654	0.583	[kpc]

the Milky Way’s thick disc. The models for the host and satellite galaxies consist of two fully self-consistent components: a dark matter (DM) halo following a NFW profile (Navarro, Frenk & White 1996), a stellar disc for the host, and a bulge for the satellite system. The stellar disc follows an exponential density profile, and the satellite’s bulge a Hernquist profile (Hernquist 1990). The properties of the Milky Way-like host and the satellite systems were scaled to those expected at $z = 1$ following Mo, Mao & White (1998). As described by Brooks et al. (2011), in this picture gas in a halo conserves its specific angular momentum (equal to that of the dark matter) as it cools to form a centrifugally supported disc that grows from the inside out. In the simplest model, in which the density profile of the galaxy is modelled as a singular isothermal sphere, the radius of the resulting disc is proportional to the parent halo virial radius. Thus, in a Λ -CDM cosmology, this would imply a decrease in the disc size of a factor of 1.7 out to $z = 1$. Later studies have shown that the evolution of the disc size - stellar mass relation predicted by this model is considerably stronger than what observations are suggesting (see e.g. Somerville et al. 2008). Note however that the results presented in this work are not strongly dependent on the particular value chosen for the host disc’s scale-length.

Both disc and bulge are represented with 1×10^5 N -body particles. To study the impact that mergers of different total mass ratios have on the phase-space structure of the disc, three different values of $f = M_{\text{host}}^{\text{tot}}/M_{\text{sat}}^{\text{tot}}$ were explored. These are $f = 20\%$, 15% , and 10% . Table 1 summarises the values of the parameters involved in these models. Note that f also sets $M_{\text{host}}^{\text{DM}}/M_{\text{sat}}^{\text{DM}}$ and $M_{\text{host}}^{\text{stellar}}/M_{\text{sat}}^{\text{stellar}}$.

The following is a brief summary of the evolution of the merger simulations analysed in this study. We refer the interested reader to VH08 for a complete description. In all cases the satellite was released from a distance of 84 kpc ($\approx 50 R_d$) from the galactic centre in the most likely infalling orbit according to previous studies on distributions of orbital parameters of infalling substructure (e.g. Benson 2005). Here R_d is the host disc’s scale-length. In such rather eccentric orbit ($e = 0.86$), the satellite rapidly reaches the

central region of the galactic halo where it is more effectively affected by dynamical friction and tidal disruption. This causes the satellite to lose orbital angular momentum, which progressively shrinks its infalling orbit. In such a way, for the simulation with $f = 20\%$, 15% , and 10% , the satellite takes roughly $t_{\text{merger}}^1 \approx 2$, 2.5 and 4 Gyr to reach and settle in the disk centre, respectively. In particular, for the $f = 20\%$, the satellite experiences ~ 8 pericentric passages, all of them at less than 20 kpc from the disk centre. As the satellite decays in its orbits, it induces the formation of tidal arms in the disc, which carry angular momentum from the disk centre outwards. Once the satellite is brought on to the plane of the disc by dynamical friction, it transfers kinetic energy from its orbits to the disc stars, increasing their vertical motions and causing a visible thickening. By the end of the simulations the morphological, structural and kinematical properties of the thickened disc and the disrupted satellite settle down and become stable, which takes place roughly 2 Gyr after the satellites have reached the disk centre. The final scale-heights of the resulting thick disks are $\approx 5 z_0$ for $f = 20\%$ and $\approx 4 z_0$ for $f = 10\%$ (see Figure 14 of VH08). Here z_0 is the scale-height of the pre-existing thin disc.

3 TEST-PARTICLE SIMULATIONS OF AN UNRELAXED DISC

In this section we briefly review the main results presented in M09 and study how the observed substructure in the velocity space of local volumes is distributed in E - L_z space. In the top panels of Figure 1 we show, at six different times, the distribution in the u - v plane of particles located within a ring of 160 pc width centred at 7.8 kpc from the disc centre. Note that the simulation is axisymmetric. Thus, the rings can be regarded as local volumes. As a consequence of the sudden energy kick imparted on the initially relaxed disc, a radial oscillation is excited on the disc particles. The radial frequency of these orbits will depend on both their orbital energies and angular momenta (see M09). Thus, particles with different energies will have different radial frequencies. These differences in frequencies induce phase-wrapping in velocity space: at a given time after the perturbation, in a given volume of space, we will observe groups of particles that have completed a different number of radial oscillations. Each one of these groups will have a characteristic frequency or energy. These groups can be observed in the u - v plane as distinct arc-like features. Note that, as time passes by and the disk relaxes, the arcs get closer together and their number increases. The bottom panels of Fig. 1 show the same distribution of particles now projected onto E - L_z space. Particles that previously were part of a given arc in the u - v plane are now distributed along well-defined features of nearly constant energy. Due to the wide range covered in the v velocity component, each arc is stretched along the L_z direction. Note that, within a volume as small

as the one considered here, the gravitational potential, $\Phi(r)$, can be regarded as a constant. Thus, for groups of particles with approximately constant energy,

$$v^2 + u^2 = 2(E - \Phi(r)) \approx cst,$$

which explains the arc-like shape of the features observed in the u - v plane.

As pointed out by M09, due to the differential rotation of the galactic disc, the separation between arcs in the u - v plane depends on the galactocentric distance of the volume under study. Increasing the size of this volume, and thus sampling a larger range of galactocentric radii, causes the waves to interfere, wiping out most of the observed substructure in velocity space. This places strong constraints on the size of the sample of stars that can be explored to identify signatures of ringing in the solar vicinity if we use velocity space.

In Figure 2 we compare the effect of volume depth in the u - v and E - L_z planes for the same simulation and time step. The top row we show the velocity distribution of particles located inside rings with different widths. The mean galactocentric distance r_{mean} of each ring is 7.8 kpc and the maximum distance sampled from r_{mean} by these rings is specified in each panel as d_{max} . Note that, by including in our sample particles that are only at 250 pc away from r_{mean} , the waves start to interfere and the arcs in u - v to overlap. In a ring with $d_{\text{max}} = 2.5$ kpc all the substructure has been completely erased. The bottom panel of Figure 2 shows the distribution of the same sets of particles in E - L_z space. When very small local volumes are considered, i.e. $d_{\text{max}} = 0.08$ kpc, both spaces are equivalent in terms of the observed substructure. However, it is very interesting to see that even in the ring with largest $d_{\text{max}} = 2.5$ kpc substructure can be clearly observed in E - L_z space. By including particles at larger radii we include density waves at different energy levels. In addition, each wave is better defined since particles that were in a different phase of their oscillation, and thus outside the arc, are now included in the sample. Note that, as expected, the separation between density waves decreases as a function of energy, i.e., with galactocentric radius.

The results presented in this section are important for two reasons. First, by sampling relatively large local volumes, it is possible to study the properties of ringing in fully self-consistent N -body simulations, where the particle resolution is much lower than in the previous experiment. Second, future astrometric missions such as *Gaia* (Perryman et al. 2001) will provide very accurate measurements of 6D phase-space coordinates for stars located at distances as large as 2.5 kpc from the position of the Sun (see e.g. Gómez et al. 2010). Although the u - v plane and the E - L_z space are equivalent when searching for signatures of ringing in local spheres with radii as small as 80 pc, the fraction of thick disc stars in this volume will be considerably smaller than in a sphere of 2.5 kpc radius. Note that it is in the thick disc where we would expect to find signatures of ringing, since these stars are less affected by perturbations from the Galactic bar, spiral structure or giant molecular clouds. Thus, the E - L_z space will allow us to explore much larger samples of thick disc stars from, e.g., a future *Gaia* catalog.

¹ In this work the merger time, t_{merger} , is defined as the time when the satellite runs out of orbital angular momentum. For the kind of orbits considered in this work, the oscillations between the centres of mass of both systems ceases approximately at the same time.

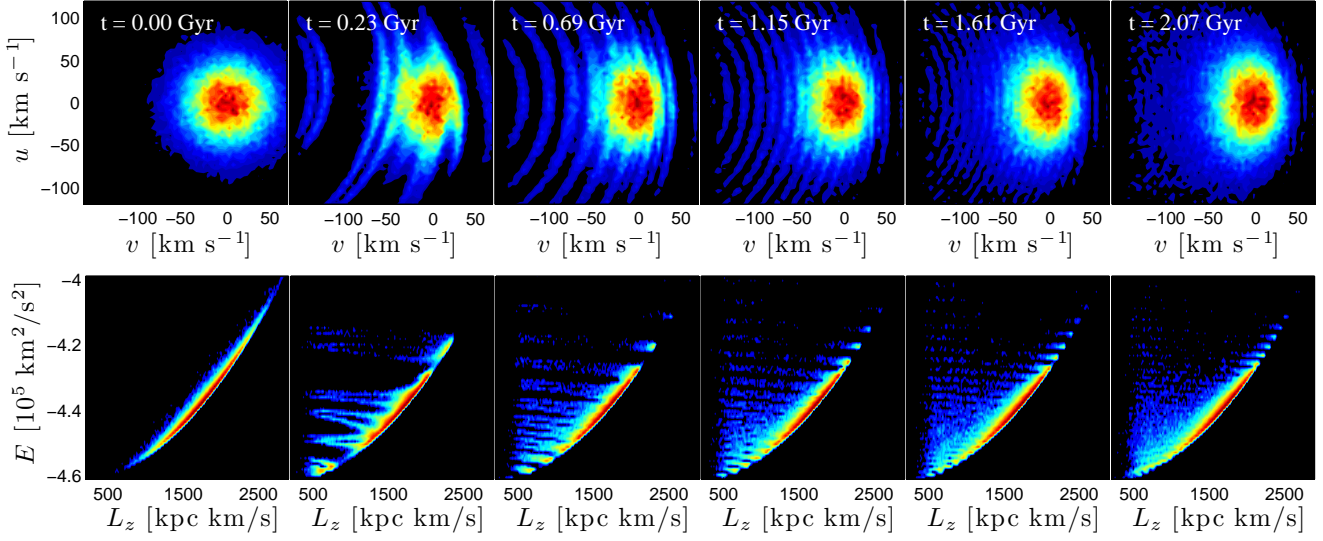


Figure 1. Distribution of particles located within a ring of 160 pc width, centred at 7.8 kpc from the galactic centre, obtained from our test-particles simulation of an unrelaxed disc. The different colours (contours) indicate different number of particles. The first column of panels shows the distribution of particles before the “merger” event. Top panels: Time development of the u - v plane distribution of particles. Note that, as explained in M09, as time passes by the number of arc-like features increases and get closer together. Bottom panels: Time development of the E - L_z distribution of particles. The substructure present in the u - v can be now observed as group of particles with approximately constant energy covering a wide range of angular momentum.

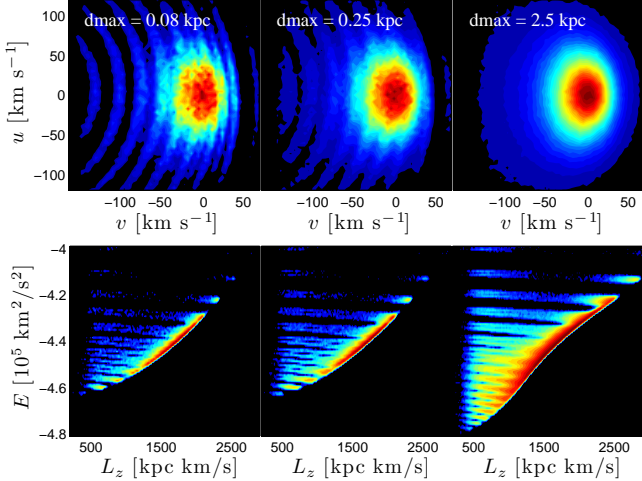


Figure 2. Distribution of particles within rings centred at 7.8 kpc from the galactic centre, obtained from our test-particles simulation of an unrelaxed disc. The different colours (contours) indicate different number of particles. Each column is associated with a ring of a different width, as indicated in the top panels. All distribution are drawn from the same snapshot, $t = 0.69$ Gyr. As the width of the ring is increased, the arcs in the u - v plane (top panels) become less clear. At $d_{\text{max}} = 2.5$ kpc substructure has been completely wiped out. Note, however, that in E - L_z space substructure can be clearly observed. As expected, the number of features in this space increases with increasing d_{max} . Note as well that the separation between energy waves decreases as a function of energy (see text).

4 FULLY SELF-CONSISTENT N -BODY SIMULATIONS

We now explore fully self-consistent N -body simulations of minor merger events. As described by VH08, the spa-

tial and kinematical structures of the pre-existing thin disc are strongly affected by the merger event. As the satellite decays in its orbit, it passes through the plane of the disc several times. At each passage, disc particles are impulsively heated by the satellite’s potential (see e.g., Quinn, Hernquist & Fullagar 1993, VH08). One manifestations of this heating mechanism is the formation of transient, non-self-gravitating spiral arms (see e.g. Tutukov & Fedorova 2006; Oh et al. 2008). The right panel of Figure 3 shows a contour plot of the distribution of particles in the X - Y plane of our $f = 20\%$ simulation, 1 Gyr after t_{merger} . It is very interesting to compare this distribution with the one obtained from the test-particles simulation, shown in the left panel of the same figure. Since the energy kick imparted on the test-particles is axisymmetric annular features (left panel) rather than spiral arms (right panel), can be observed. It is important to emphasise that the spiral features observed in our N -body simulations are not self-gravitating, as they quickly disappear with time. This can also be inferred from the large values of the radial velocity dispersion of the resulting thick disc shown in Figure 4. In this figure we show the radial velocity dispersion profile of the disc at three different times. The radial velocity dispersion is considerably larger at all radii already 0.1 Gyr after the satellite galaxy is fully merged. This profile does not evolve significantly during the next 2.9 Gyr of simulation. Within 5 to 10 kpc from the disc centre, the radial velocity dispersion takes a value of $\sigma_u \approx 50 \text{ km s}^{-1}$, which is consistent with the value used in the test-particles simulation. As expected, the asymmetric drift induced in this way causes a decrease in the rotational velocity as a function of radius after the merger. Note that, although its magnitude decreased by about 20% at $R \geq 4$ kpc, a flat profile is preserved. We will now analyse solar-neighbourhood-like

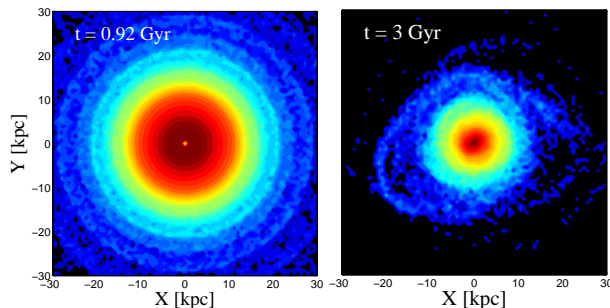


Figure 3. Left panel: Distribution of particles in the X - Y plane, as obtained from our test-particles simulation of an unrelaxed disc, ≈ 1 Gyr after the energy kick. The different colours (contours) indicate different number of particle. Note the multiple annular features, associated with density waves. Right panel: Distribution of particles in the X - Y plane 1 Gyr after t_{merger} ($t = 3$ Gyr), as obtained from our N -body simulation of a merger event with a mass ratio of $f = 20\%$. As a consequence of the non-axisymmetrical energy kick imparted by the satellite as it crosses the plane of the disc, spiral features (rather than annular) are formed.

volumes in the resulting thick disc, to search for signatures of ringing in energy and angular momentum space.

4.1 Density waves in E - L_z space

Since the particle resolution of these simulations is much lower than that of our test-particles simulation, it is not feasible to look for signatures of density waves in volumes as small as the ones analysed in Section 3. In what follows, we focus our analysis on samples of particles located within spheres of 2.5 kpc radius. The simulations analysed in this work were designed to emulate the result of a minor merger experienced by a Milky Way-like galaxy at $z = 1$. Therefore, the scales of our final thick disc are relatively smaller compared to those observed in the Milky Way. As explained by Villalobos & Helmi (2009), it is not straightforward to decide which radii corresponds to a solar neighbourhood-like volume. Following their work, we place our sphere at two different locations, namely 5.5 kpc ($\sim 2.4R_{\text{td}}$) and 8 kpc ($\sim 3.5R_{\text{td}}$), where $R_{\text{td}} = 2.28$ kpc is the final scale length of the simulated thick disc. This also allows us to study the expected dependance of the number and distribution of density waves with galactocentric radius.

The left panel of Figure 5 shows the distribution in the $u-v$ plane of particles that are located inside a sphere centred at (8,0,0) kpc from the galactic centre, 0.7 Gyr after t_{merger} ². This distribution was obtained from our $f = 20\%$ simulation. Note that only 865 disc particles are found within this sphere. Due to the large volume sampled, the absence of arc-like features in this projection of phase-space is not surprising. The same distribution of particles projected in E - L_z space is shown on the right panel of this figure. Interestingly, particles are now distributed in well-defined clumps of approximately constant energy.

² This particular time and location were chosen arbitrarily for simplicity. Dependencies with azimuthal angles are explored in Section 4.2

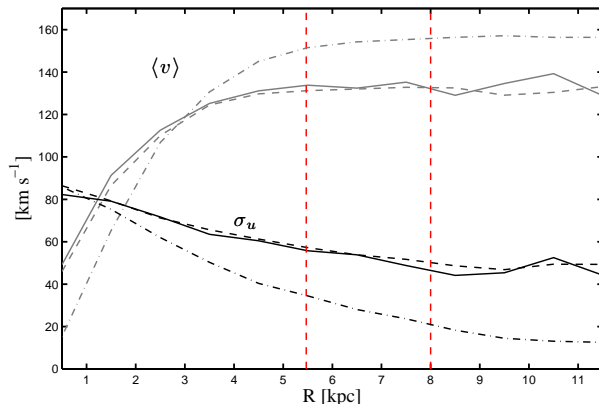


Figure 4. Radial velocity dispersion and mean azimuthal velocity profiles at three different times, from our $f = 20\%$ N -body simulation. The profiles have been computed within concentric rings of 1 kpc width for particles with $|Z| < 1.5$ kpc. The solid and dashed lines show the profiles computed at $t = 2.1$ and 4.5 Gyr, which corresponds to 0.1 and 2.5 Gyr after t_{merger} , respectively. The dotted dashed lines represent both profiles at $t = 0$ Gyr. Note that the later were obtained after evolving the host for 3 Gyr in isolation. The red vertical lines indicate the positions of the spheres studied in Section 4.1

Each clump represents a different density wave crossing the sphere. Figure 6 shows the time evolution of this distribution. Note that our solar neighbourhood-like volume is rotating with an angular frequency set by the velocity of the local standard of rest (LSR), obtained after correcting the final mean rotational velocity profile for axisymmetric drift (Noordermeer, Merrifield & Aragón-Salamanca 2008). Over time, the number of clumps increases and they come closer together, as expected from Section 3 (see also M09). Substructure can be clearly observed already at $t \approx 0.8$ Gyr and can be followed until $t \approx 4.7$ Gyr, spanning a total of about 4 Gyr. Later, although still present, the signatures of the density waves are difficult to observe even in E - L_z space. Recall that for this simulation, $t_{\text{merger}} \approx 2$ Gyr. Thus, substructure can be observe in the E - L_z plane for about 2.7 Gyr after the satellite has completely “sunk” to the centre of the host’s disc. Figure 7 shows, as a function of time, the E - L_z distribution of the particles located inside the sphere centred at 5.47 kpc from the galactic centre. Again, a wealth of substructure can be observed. Comparison of this figure with Figure 6 reveals the presence of a larger number of clumps at any given time after t_{merger} . This reflects the dependance of the phase-mixing time-scale on galactocentric distance (see M09). Note that in this inner sphere the perturbation is triggered after ~ 1.1 Gyr, a time that corresponds to the second pericentric passage (and thus, closer to the galactic centre) of the satellite galaxy. Substructure can be clearly observed for a total of ≈ 2.8 Gyr, and for ≈ 1.9 Gyr after t_{merger} .

We have also analysed a self-consistent simulation of a galactic disk evolved in isolation. The disc is first relaxed within a rigid version of the halo potential for about 1 Gyr. Once the disc is relaxed the rigid halo is replaced by its N -body counterpart and the system is evolved fully self-consistently for 4 Gyr (See VH08, Section A3 for a detailed description of this procedure). Even after 4 Gyr of evolu-

tion, no noticeable substructure can be observed in the E - L_z distribution of particles located within solar neighbourhood-like volumes.

4.2 Azimuthal dependance

As opposed to the axisymmetric energy kick imparted to our test-particle simulation, the merging satellite galaxy is expected to impulsively heat the disc in a preferential direction associated with its orbit. Therefore, we would expect to observe a phase difference in the distribution of substructure observed in solar neighbourhood-like volumes located at different azimuthal angles. To explore this, we follow in our $f = 20\%$ simulation the E - L_z distribution of the particles enclosed within four different spheres for ~ 1 Gyr. The spheres are located at $(\pm 8, 0, 0)$ kpc and $(0, \pm 8, 0)$ kpc and hereafter we will refer to them as $x = \pm 8$ kpc and $y = \pm 8$ kpc. For this particular analysis we keep the sphere fixed at their initial locations. The results are shown in Figure 8. Each row of panels shows the time evolution of this distribution on a different sphere. The panels are labelled, in the leftmost column, according to the position of the corresponding sphere. At any given time, the distribution of substructure in E - L_z space is different from sphere to sphere. A visual inspection of the first column of panels indicates a larger fraction of substructure on the $y = -8$ kpc sphere, 0.1 Gyr after t_{merger} . Note that this direction corresponds with the direction of the first *close* passage of the satellite through the galactic disc, as shown by Figures 1 and 2 in VH08. It is also noticeable that the distribution of particles repeats itself along diagonals starting from bottom left to top right panels. This implies that the phase difference of the density wave can be well described as an spiral pattern, travelling approximately an angle of $\frac{3}{2}\pi$ radians in 0.2 Gyr, in agreement with the spatial distribution of disc particles observed in Figure 3. To examine this, let us estimate the averaged angular period of a particle located at 8 kpc from the galactic centre. From Figure 4, at $r = 8$ kpc, $\langle v \rangle \approx 130$ km s $^{-1}$. Thus,

$$T_\phi = \frac{2\pi r}{\langle v \rangle} \approx 0.38 \text{ Gyr},$$

implying that in 0.2 Gyr, particles have travelled approximately an angle π through the disc. As a consequence, the ratio between the angular and the radial frequencies³ of the particles located inside our sphere is expected to be

$$\frac{\Omega_\phi}{\Omega_r} \approx \frac{2}{3}.$$

Figure 9 shows the distribution of orbital frequencies of the particles located inside the $x = +8$ kpc sphere, 0.7 Gyr after t_{merger} . The frequencies were computed as described in Gómez & Helmi (2010, hereafter GH10) and we refer the reader to their work for a detailed description of their estimation method (see also Carpintero & Aguilar 1998). Note that particles tend to lie on the curve $\Omega_\phi = 2.1\Omega_r/3$, in good agreement with our previous discussion. It is very interesting to observe that, in frequency space, particles are also

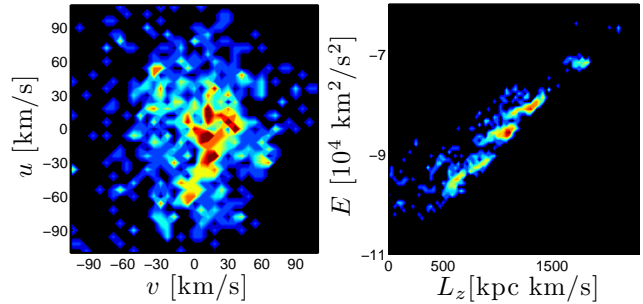


Figure 5. Distribution of disc particles inside a sphere of 2.5 kpc radius located at 8 kpc from the centre, obtained from our N -body simulation with a mass ratio of $f = 20\%$, 0.7 Gyr after t_{merger} . The left panel shows the distribution of particles in velocity space whereas the right panel corresponds to the E - L_z projection. Note that, unlike in velocity space, a large number of substructures can be observed in E - L_z space.

distributed in well-defined lumps representing the different density waves crossing the volume.

4.3 Dependence on satellite's mass

It is well known that the amount of disc heating induced by a merger event strongly depends on the properties of the merging satellite, such as its concentration and total mass (see, e.g., Quinn, Hernquist & Fullagar 1993; Benson et al. 2004; Di Matteo et al. 2011, VH08). Although, since $z = 1$, mergers with mass ratios as large as 20% are likely to occur in galaxies such as the Milky Way, the likelihood of these events increases with decreasing mass ratios (see e.g. De Lucia & Helmi 2008; Kazantzidis et al. 2009; Cooper et al. 2010). It is therefore interesting to study whether perturbations induced by less massive minor mergers can leave imprints on the phase-space distribution of galactic disc stars. In this section we investigate minor merger events with mass ratios of $f = 15\%$ and 10% . Table 1 summarises the main properties of both satellites. For less massive satellites than those considered here, dynamical friction is expected to be less efficient. Thus, this kind of satellites are unlikely to reach the centre of the host system and to cause significant changes in its structure (VH08, Binney & Tremaine 2008; Kazantzidis et al. 2009).

Figure 10 shows, for both simulations, the time evolution of the E - L_z distribution of particles located inside a sphere centred at 8 kpc from the galactic centre⁴. Both spheres are rotating with an angular frequency derived from the corresponding velocity of their LSR. Interestingly, even for the simulation with a mass ratio $f = 10\%$ (bottom panels), substructure can be clearly observed in the phase-space distribution of disc stars for a period of about 4 Gyr. This is approximately the same period of time that we were able to follow substructure in our $f = 20\%$ simulation. This can be explained as follows: Although the strength of the perturbation on the host's disc depends on satellite's mass, lower-mass satellites take longer to completely sink onto the

³ Note that most of these particles have very low eccentricities and thus $\kappa \approx \Omega_r$, where κ represents the epicyclic frequency

⁴ Note that, as shown in Figure 14 of VH08, the final thick disc's scale length of the $f = 10\%$ simulation does not significantly differ from the one measured on the $f = 20\%$ simulation.

galactic centre. For example, in our $f = 10\%$ simulation $t_{\text{merger}} \approx 4$ Gyr. As a consequence, a lower mass satellite can excite the galactic disc for a longer period of time (see also Quillen et al. 2009). Note however that, after t_{merger} , substructure can be followed only for ~ 2.3 and ~ 0.9 Gyr for the simulation with $f = 15\%$ and 10% , respectively. Low mass satellites generates density waves with smaller amplitudes and thus, their signatures after t_{merger} disappear faster as they quickly get within the noise level.

4.4 Contamination from satellite's debris

In the analysis carried out so far, only particles from the galactic disc were taken into account. As described by VH08, a large fraction of the particles from the satellite ends up in a disc-like configuration, with the same spatial orientation as the final thick disc. Therefore, the distribution of the satellite's particles in E - L_z space could partially overlap with the corresponding distribution of disc particles, complicating the detection of density waves.

The distribution of debris left by a satellite on a solar neighbourhood-like sphere, obtained from a simulation similar to the ones considered here, was already studied in detail by GH10. The only difference between their $f = 20\%$ simulation and ours is the particle resolution of the satellite galaxy. To enhance the signatures of stellar streams, the satellite analysed by GH10 was modelled with a number of particles ten times larger than the one used here (see also VH08). Figure 13 of GH10 shows the distribution of particles from both systems, in four different projections of phase-space. Not surprisingly, for a given energy, particles from the satellites tend to have smaller angular momentum than those from the disc (see bottom middle panel). Even in this simulation with a much higher satellite's resolution, substructure from the disc can be easily identified in E - L_z space. Note as well that substructure in the disc can be clearly observed in apocentre vs. pericentre space (bottom left panel).

5 SUMMARY AND CONCLUSIONS

In this work we have explored the impact that minor mergers have on the phase space distribution of a galactic stellar disc, such as the one in the Milky Way. Using numerical simulations, we showed that the pseudo-integrals of motion E - L_z space is well-suited to identify density waves in the disc's velocity field that have been generated by the merger event. In this space, particles in a given volume of physical space are distributed along features of nearly constant energy, each associated with a different wave. The separation between density waves at different energy levels indicates the time since the disc was perturbed by the merging satellite. Interestingly, substructure in E - L_z space can be clearly observed even when solar neighborhood-like spheres with radii as large as 2.5 kpc are considered. This is in stark contrast with what is observed in the u - v plane, where the waves inside spheres with radii larger than ~ 0.25 kpc interfere, wiping out all signatures of ringing. An important implication of this result is that a larger sample of stars could be explored to search for signatures of minor merger events in the Milky Way thick disc. This is relevant not only in the

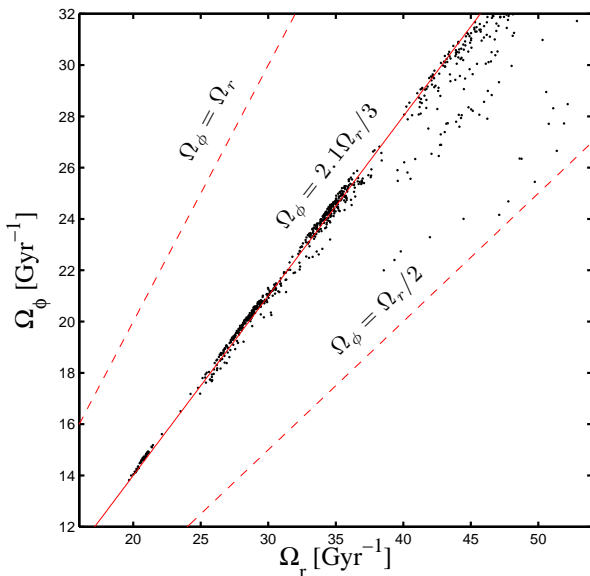


Figure 9. Distribution in frequency space of disc particles inside a sphere of 2.5 kpc radius located at 8 kpc from the galactic centre, obtained from our N -body simulation with a mass ratio of $f = 20\%$, 0.7 Gyr after t_{merger} . Note that substructure can be easily identify as well in this space. The solid line indicates the ratio between frequencies of disc particles, whereas the dashed lines denote the limits of this space.

context of the forthcoming full 6D phase space *Gaia* catalog, but also for available catalogs, such as those provided by RAVE (see, e.g., Breddels et al. 2010) and SDSS (Lee et al. 2011).

By projecting the distribution of particles located inside spheres of 2.5 kpc radius onto E - L_z space we were able, for the first time, to study the properties of ringing in fully self-consistent N -body simulations of disc galaxies minor mergers. We showed that, in a simulation of a merger between a satellite galaxy and a host disc with a mass ratio $f = 20\%$, signatures of ringing can be clearly observed for a total of ~ 4 Gyr and for about 2.7 Gyr after the merger has concluded. It is remarkable that the $\lesssim 1000$ particles enclosed in our local volumes were enough to resolve a wealth of substructure in the resulting thick disc. In addition, we showed that the in-fall trajectory of the perturber satellite gives rise to an azimuthal dependence of the structure observed in E - L_z space. Note that we have only explored distributions of particles in this pseudo-integrals of motion space. Information about orbital properties of the merging satellite, such as its in-fall trajectory or its impact parameter, could be obtained by exploring the distributions of particles' angular phases as a function of galactocentric azimuthal angle. This will be analyse in a follow-up study.

We have also explored the impact that mergers of different total mass ratios have on the phase-space structure of the disc. Interestingly, mergers with mass ratios as small as $f = 10\%$ give rise to density waves in the velocity field of the disc that can also be followed for a total of ~ 4 Gyr. This is a consequence of the longer period of time required by a lower mass satellite to fully merge with its host. On the other hand, once the merger concludes substructure can be followed for only ~ 0.9 and ~ 2.3 Gyr for simulations with mass

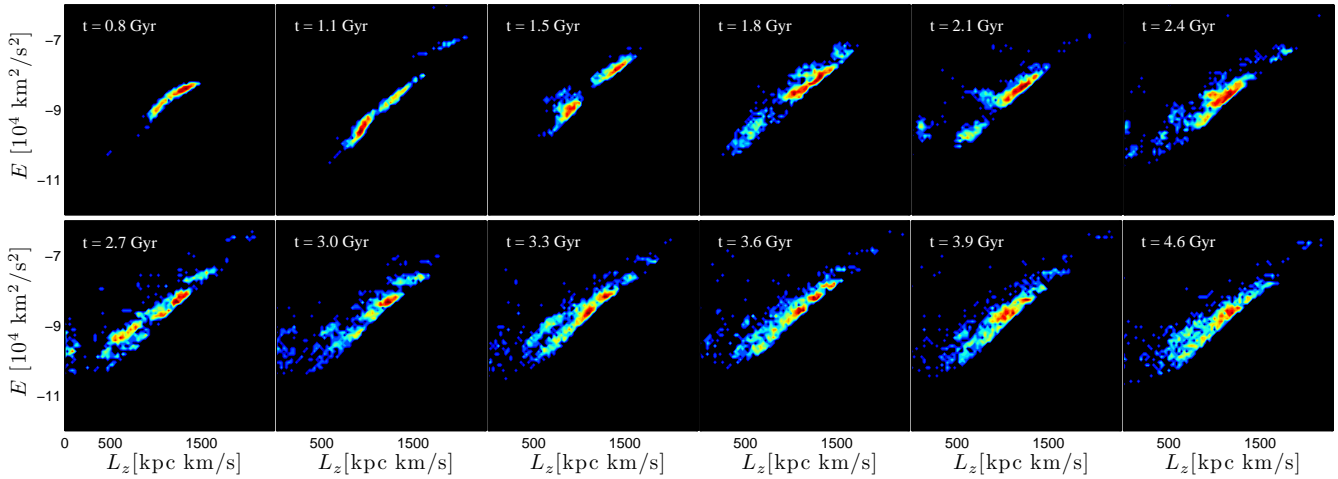


Figure 6. Time development of the E - L_z space for a distribution of particles located within a sphere of 2.5 kpc centred at 8 kpc from the galactic centre, obtained from our N -body simulation with a mass ratio of $f = 20\%$. The sphere is rotating with an angular velocity set by the velocity of the LSR. Note that, as expected, the number of lumps associated with density waves increases as time passes by. Substructure can be clearly observed for a total of ~ 4 Gyr. In this simulation the merger concludes at $t_{\text{merger}} \approx 2$ Gyr.

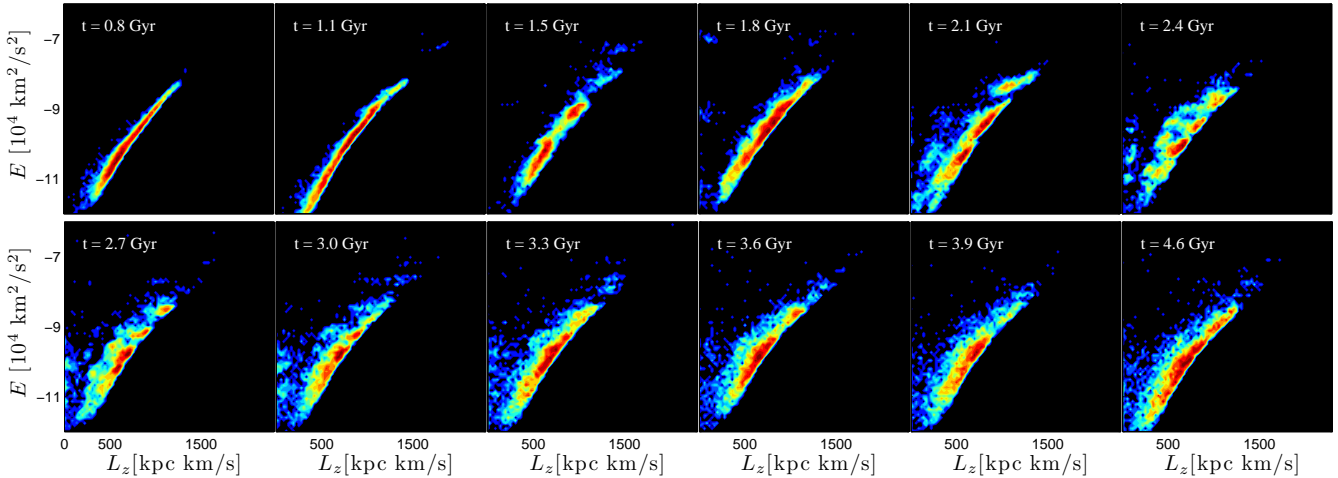


Figure 7. As in Figure 6 for particles located within a sphere centred at 5.47 kpc from the galactic centre. Note that mixing occurs more rapidly than in our sphere centred at 8 kpc, reflecting the dependance of the mixing time-scale on galactocentric radius. In this sphere, substructure can be clearly observe for a total of to ~ 2.8 Gyr. In this simulation the merger concludes at $t_{\text{merger}} \approx 2$ Gyr.

ratio of $f = 10$ and 15% , respectively. Note that these results are constrained by the low particle resolution of our N -body simulations; higher resolution simulations could allow us to follow substructure for longer periods of time. Thus, signatures of minor merger that have evolved for longer than 4 Gyr could be identified from the very large and accurate sample of thick disc stars that soon will become available thanks to *Gaia*.

M09 showed that a merger event ≈ 1.9 Gyr ago could not only explain the high velocity streams seen in the Solar Neighbourhood at approximate v of -60 (HR 1614, Eggen 1992), -80 (Arifanto & Fuchs 2006), -100 (Arcturus), and -160 km/s (Klement, Fuchs & Rix 2008) but also predicts four new high velocity streams at $v \approx 140$, -120 , 40 and 60 km/s. By selecting samples of thick disc stars (Nordström et al. 2004; Schuster et. al. 2006) they found indications of these new streams in velocity space. However, their results are not statistically significant since, due to

the constraints on the size of the local volume ($d_{\text{max}} = 0.08$ & 0.15 kpc), samples of only 451 and 766 stars were explored. We are currently analysing the aforementioned 6D phase space catalogs from RAVE and SDSS to search for signatures of these streams in E - L_z space.

ACKNOWLEDGMENTS

We would like to thank Alice Quillen for helpful comments. FAG was supported through the NSF Office of Cyberinfrastructure by grant PHY-0941373, and by the Michigan State University Institute for Cyber-Enabled Research. BWO was supported in part by the Department of Energy through the Los Alamos National Laboratory Institute for Geophysics and Planetary Physics.

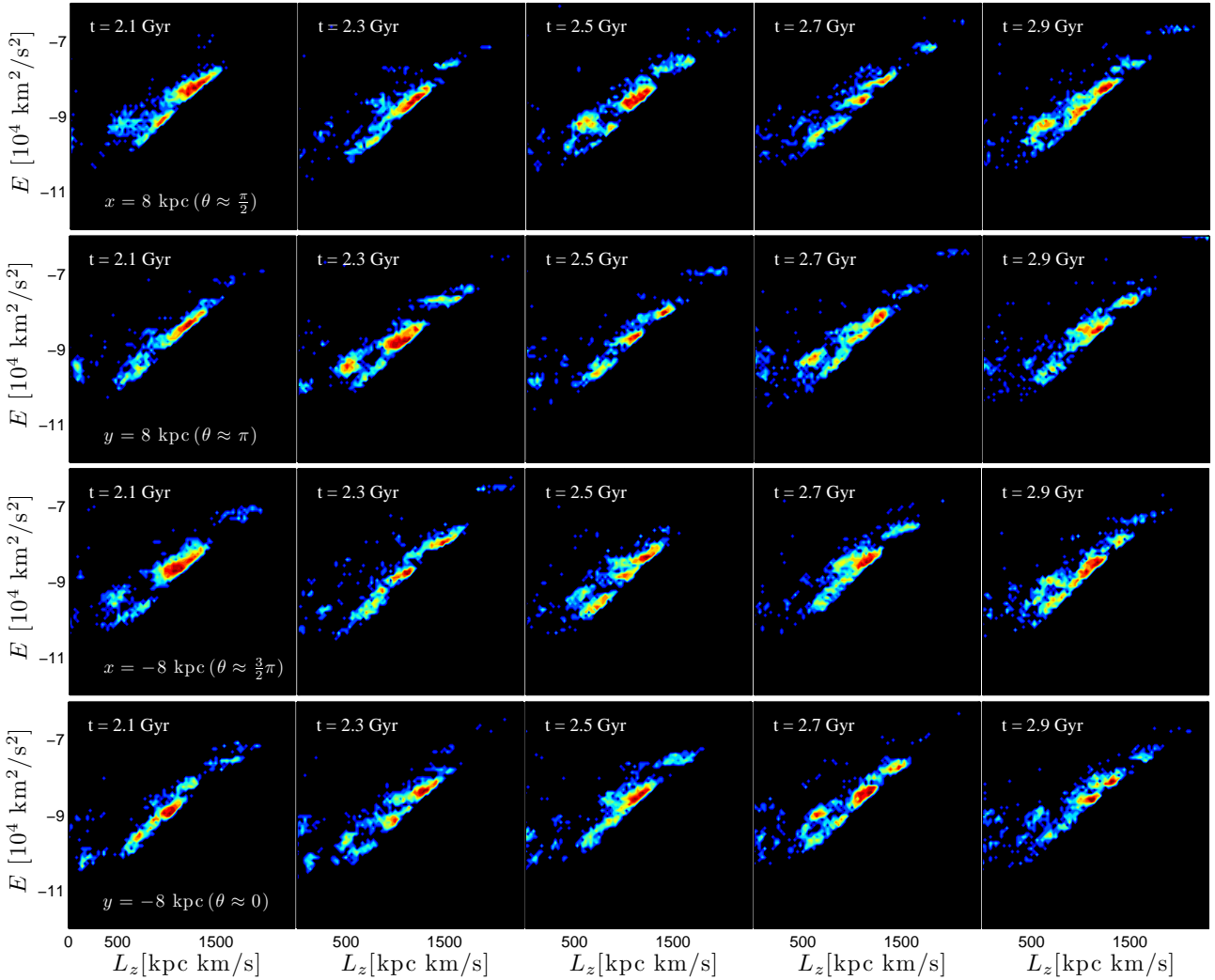


Figure 8. Azimuthal dependance on the distribution of lumps in E - L_z space. Each row of panel shows the time development of the distribution of disc particles inside a different sphere, obtained from our N -body simulation with a mass ratio of $f = 20\%$. The location of the spheres are indicated on the panel's bottom left corner of each panel. The variable θ approximately indicates the angle with respect to the direction of the first close passage of the satellite through plane of the disc. The spheres are kept fixed in their initial locations. Note that, along diagonals starting from bottom left to top right panels, the distribution of particles approximately repeats itself. This indicates both, a phase difference on the density waves at different azimuthal angles and a relation between angular and radial frequencies of disc particles.

REFERENCES

- Antoja T., Valenzuela O., Pichardo B., Moreno E., Figueras F., Fernández D., 2009, *ApJ*, 700, L78
 Arifanto M. I., Fuchs B., 2006, *A&A*, 449, 533
 Belokurov V. et al., 2006, *ApJ*, 642, L137
 Benson A. J., Lacey C. G., Frenk C. S., Baugh C. M., Cole S., 2004, *MNRAS*, 351, 1215
 Benson A. J., 2005, *MNRAS*, 358, 551
 Binney J., Tremaine S., 2008, *Galactic Dynamics*. Princeton Univ. Press, Princeton, NJ
 Breddels M. A., et al., 2010, *A&A*, 511, A90
 Brooks, A., et al., 2011, *ApJ*, 728, 51
 Bullock J. S., Johnston K. V., 2005, *ApJ*, 635, 931
 Carpinero D. D., Aguilar L. A., 1998, *MNRAS*, 298, 1
 Cooper A. P. et al., 2010, *MNRAS*, 406, 744
 Chapman S. C. et al., 2008, *MNRAS*, 390, 1437
 De Lucia G., Helmi A., 2008, *MNRAS*, 391, 14
 Dehnen W., 2000, *AJ*, 119, 800
 Di Matteo P., Lehnert M. D., Qu Y., van Driel W., 2011, *A&A*, 525, L3
 Eggen O. J., 1996, *AJ*, 112, 1595
 Eggen O. J., 1992, *AJ*, 104, 1906
 Font A. S., Johnston K. V., Bullock J. S., Robertson B. E., 2006, *ApJ*, 646, 886
 Fux, R., 2001, *A&A*, 373, 511
 Freeman K., Bland-Hawthorn J., 2002, *ARA&A*, 40, 487
 Gómez F. A., Helmi A., 2010, *MNRAS*, 401, 2285
 Gómez F. A., Helmi A., Brown A. G. A., Li Y. S., 2010, *MNRAS*, 408, 935
 Helmi A., de Zeeuw P. T., 2000, *MNRAS*, 319, 657
 Helmi A., White S. D. M., 1999, *MNRAS*, 307, 495
 Helmi A., White S. D. M., de Zeeuw P. T., Zhao H., 1999, *Nature*, 402, 53
 Helmi A., Navarro J. F., Nordström B., Holmberg J., Abadi

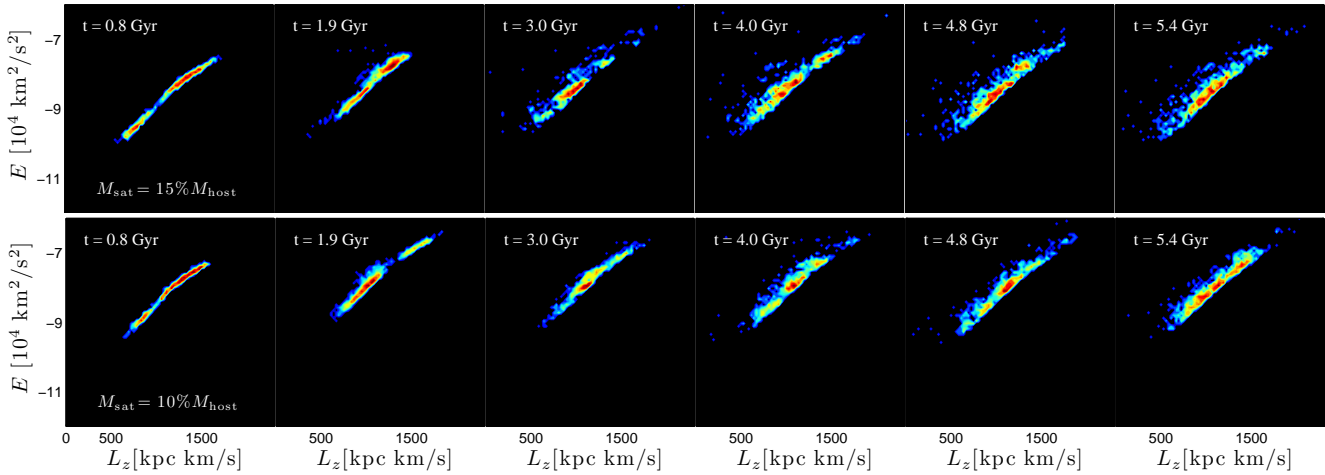


Figure 10. Time development of the distribution of disc particles located within a sphere in $E - L_z$ space, obtained from two N -body simulations of mergers with mass ratios $f = 15\%$ (top panels) and 10% (bottom panels). The sphere is centred at 8 kpc from the galactic centre and has a radius of 2.5 kpc. In both simulations, substructure can be followed for a total of ~ 4 Gyr. The merger concludes at $t_{\text{merger}} \approx 2.5$ and 4 Gyr for the simulation with $f = 15\%$ and $f = 20\%$, respectively.

M. G., Steinmetz M., 2006, MNRAS, 365, 1309
Hernquist L., 1990, ApJ, 356, 359
Ibata R., Irwin M. J., Lewis G. F., Ferguson A. M. N., Tanvir N., 2003, MNRAS, 340, L21
Ibata R. A., Irwin M. J., Lewis G. F., Ferguson A. M. N., Tanvir N., 2001a, Nature, 412, 49
Ibata R. A., Gilmore G., Irwin M. J., 1994, Nature, 370, 194
Kazantzidis S., Zentner A. R., Kravtsov A. V., Bullock J. S., Debattista V. P., 2009, ApJ, 700, 1896
Klement R., Fuchs B., Rix H.-W., 2008, ApJ, 685, 261
Klement R. et al., 2009, ApJ, 698, 865
Lee Y. S., et al., 2011, ApJ, 738, 187
Martínez-Delgado D., Pohlen M., Gabany R. J., Majewski S. R., Peñarrubia, J., Palma C., 2009, ApJ, 692, 955
Martínez-Delgado D., Peñarrubia J., Gabany R. J., Trujillo I., Majewski S. R., Pohlen M., 2008, ApJ, 689, 184
McConnachie A. W. et al., 2009, Nature, 461, 6673
Michel-Dansac L., Abadi M. G., Navarro J. F., Steinmetz M., 2011, MNRAS, 414, L1
Minchev I., Boily C., Siebert A., & Bienayme O., 2010, MNRAS, 407, 2122
Minchev I., Quillen A. C., Williams M., Freeman K. C., Nordhaus J., Siebert A., Bienayme O., 2009, MNRAS, 396, L56
Minchev I., Quillen A. C., 2008, MNRAS, 386, 157
Mo H. J., Mao S., White S. D. M., 1998, MNRAS, 295, 319
Navarro J. F., Frenk C. S., White S. D. M., 1996, ApJ, 462, 563
Navarro J. F., Helmi A., Freeman K. C., 2004, ApJL, 601, L43
Newberg H. J. et al., 2002, ApJ, 569, 245
Nordström B., Mayor M., Andersen J., Holmberg J., Pont F., Jørgensen B. R., Olsen E. H., Udry S., Mowlavi N.: 2004, 2004, A&A, 418, 989
Noordermeer E., Merrifield M. R., Aragón-Salamanca, A. 2008, MNRAS, 388, 1381
Oh S. H., Kim W.-T., Lee H. M., Kim J., 2008, ApJ, 683, 94

Perryman M. A. C. et al., 2001, A&A, 369, 339
Quillen A. C., Minchev I., Bland-Hawthorn J., Haywood M., 2009, MNRAS, 397, 1599
Quillen A. C., Dougherty J., Bagley M. B., Minchev I., Comparetta J., 2011, MNRAS, 417, 762
Quinn P. J., Hernquist L., Fullagar D. P., 1993, ApJ, 403, 74
Sales L. V., et al. 2008, MNRAS, 389, 1391
Schuster W. J., Moitinho A., Márquez A., Parrao L., Covarrubias E., 2006, A&A 445, 939
Somerville R. S., et al., 2008, ApJ, 672, 776
Starkenburg E. et al., 2009, ApJ, 698, 567
Tutukov A. V., Fedorova A. V., 2006, Astron. Rep., 50, 785
Yanny B. et al., 2003, ApJ, 588, 824
Villalobos A., 2009, Ph.D. thesis, University of Groningen
Villalobos A., Helmi A., 2009, MNRAS, 399, 166
Villalobos A., Helmi A., 2008, MNRAS, 391, 1806
Williams M. E. K., et al., 2011, ApJ, 728, 102
Williams M. E. K., Freeman K. C., Helmi A., the RAVE collaboration, 2009, in IAU Symp. 254, The Galaxy Disk in Cosmological Context, ed. J. Andersen, J. Bland-Hawthorn, & B. Nordström, (Cambridge: Cambridge Univ. Press), 139